Superconducting Fluctuations in Overdoped $Bi_2Sr_2CaCu_2O_{8+\delta}$

Yu He,[1,2,3,4,*] Su-Di Chen,[1,3,*] Zi-Xiang Li,[2,*] Dan Zhao,[5,6] Dongjoon Song,[7] Yoshiyuki Yoshida,[7] Hiroshi Eisaki,[7] Tao Wu,[5,6] Xian-Hui Chen,[5,6] Dong-Hui Lu,[8] Christoph Meingast,[9] Thomas P. Devereaux,[10,3] Robert J. Birgeneau,[2,4] Makoto Hashimoto,[8] Dung-Hai Lee,[2,4] and Zhi-Xun Shen[1,3]

[1]*Department of Applied Physics, Stanford University, Stanford, California 94305, USA*
[2]*Department of Physics, University of California at Berkeley, Berkeley, California 94720, USA*
[3]*Stanford Institute for Materials and Energy Sciences, SLAC National Accelerator Laboratory, 2575 Sand Hill Road, Menlo Park, California 94025, USA*
[4]*Materials Sciences Division, Lawrence Berkeley National Laboratory, Berkeley, California 94720, USA*
[5]*Hefei National Laboratory for Physical Sciences at the Microscale, University of Science and Technology of China, Hefei, Anhui 230026, China*
[6]*CAS Key Laboratory of Strongly-coupled Quantum Matter Physics, Department of Physics, University of Science and Technology of China, Hefei, Anhui 230026, China*
[7]*National Institute of Advanced Industrial Science and Technology, Tsukuba 305-8565, Japan*
[8]*Stanford Synchrotron Radiation Lightsource, SLAC National Accelerator Laboratory, Menlo Park, California 94025, USA*
[9]*Institute for Quantum Materials and Technologies, Karlsruhe Institute of Technology, 76021 Karlsruhe, Germany*
[10]*Department of Materials Science and Engineering, Stanford University, Stanford, California 94305, USA*

(Received 16 April 2021; revised 15 June 2021; accepted 26 July 2021; published 28 September 2021)

Fluctuating superconductivity—vestigial Cooper pairing in the resistive state of a material—is usually associated with low dimensionality, strong disorder, or low carrier density. Here, we report single-particle spectroscopic, thermodynamic and magnetic evidence for persistent superconducting fluctuations in the heavily hole-doped cuprate superconductor $Bi_2Sr_2CaCu_2O_{8+\delta}$ ($T_c = 66$ K) despite the high carrier density. With a sign-problem-free quantum Monte Carlo calculation, we show how a partially flat band at $(\pi, 0)$ can help enhance superconducting phase fluctuations. Finally, we discuss the implications of an anisotropic band structure on the phase-coherence-limited superconductivity in overdoped cuprates and other superconductors.

DOI: 10.1103/PhysRevX.11.031068

Subject Areas: Condensed Matter Physics, Superconductivity

I. INTRODUCTION

In conventional superconductors, the superconducting (SC) transition temperature T_c is controlled by the formation of Cooper pairs via exchange of low-energy pairing bosons of energy Ω_p in the BCS paradigm [1]. Here, the normal state has many high kinetic energy carriers ($\epsilon_F \gg \Omega_p$), and pairing happens only between quasiparticle eigenstates with well-defined energy and momentum on a thin shell around the Fermi surface. Meanwhile, with the fluctuations in the pairing field neglected, superconducting phase coherence and Cooper pairing are simultaneously established via a mean-field second-order phase transition at T_c. Thermal superconducting fluctuation is only notable near T_c within a small temperature range δT, which is dictated by the Ginzburg criteria [2]. In a three-dimensional clean metal [3], $\delta T/T_c \ll 1$ is expected theoretically and observed experimentally [4–6].

Investigations of the superconductor-to-insulator transition in superconducting thin films reveal prevailing fluctuations that are largely controlled by disorder and dimensionality [7–11]. There, higher level of disorder (measured by residual resistivity) can rapidly increase the separation between the superconducting pairing temperature T_{pair} and the zero resistance temperature T_c. The thermodynamic superconducting transition happens at T_c, where superconducting correlation length diverges, while T_{pair} becomes a crossover temperature scale that signifies the occurrence of nonzero superconducting pairing field

*These authors contributed equally to this work.

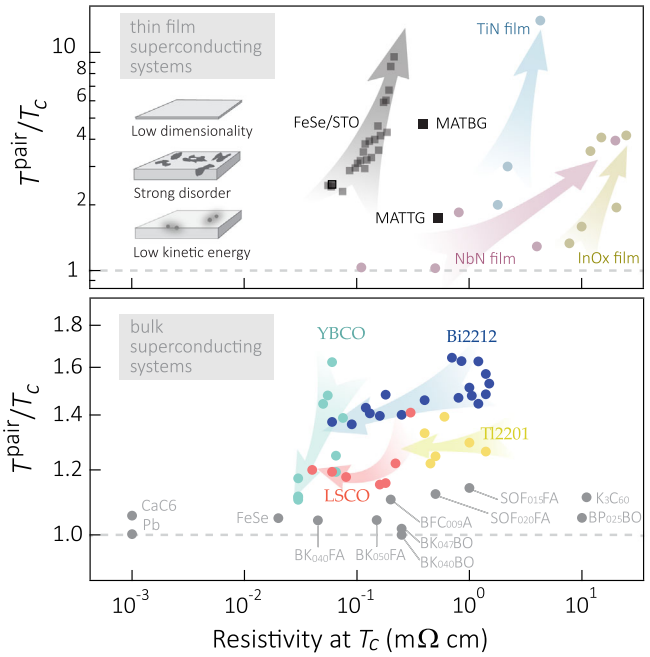

FIG. 1. Thermal superconducting fluctuation effect in conventional and unconventional superconductors. Superconducting gap opening temperature T_{pair} divided by zero resistance temperature T_c tallied according to the resistivity right above T_c for (top) thin film superconductors and (bottom) bulk superconductors. Arrows denote increasing disorder in thin film systems and increasing hole doping in the cuprates. Except for TBG and TTG systems, T_{pair} is exclusively determined from heat capacity or single-particle spectra [16]. MATBG (MATTG), magic angle twisted bilayer (trilayer) graphene; FeSe/STO, monolayer FeSe on Nb:$SrTiO_3$; BKFA, $Ba_{1-x}K_xFe_2As_2$; BFCA, $Ba(Fe_{1-x}Co_x)_2As_2$; BKBO, $Ba_{1-x}K_xBiO_3$; BPBO, $BaPb_{1-x}Bi_xO_3$; SOFFA, $SmO_{1-x}F_xFeAs$; YBCO, $YBa_2Cu_3O_{7-\delta}$; Tl2201, $Tl_2Ba_2CuO_{6+\delta}$; LSCO, $(La,Sr)_2CuO_4$; Bi2212, $Bi_2Sr_2CaCu_2O_{8+\delta}$ [16].

modulus [12]. Between T_c and T_{pair}, the phase of the superconducting order parameter remains disordered. Because of the crossover nature, experimental measures of T_{pair} may depend on the nature of the probe. In thermodynamic probes such as heat capacity, T_{pair} may be represented as the "mean-field" pairing temperature T_{MF} via equal entropy reconstruction [13]; whereas in single-particle probes, it is often signified by the spectral gap opening temperature T_{gap} [14]. Figure 1(a) aggregates the severity of superconducting fluctuations (T_{pair}/T_c) for most commonly studied 2D superconductors as a function of materials' resistivity at T_c, which is considered a measure of disorder within the same material family. It should be noted that for strictly mono-to-few atomic layer systems such as $FeSe/SrTiO_3$ or twisted graphene, T_c is always suppressed from T_{pair} due to prevalent vortex excitations even in the absence of disorder [15]. Clearly in these systems, fluctuating superconductivity can survive up to a T_{pair} several times higher than T_c. In contrast, bulk superconducting systems exhibit fluctuations to a much lesser degree [Fig. 1(b)], which is consistent with the Ginzburg criteria in mean-field superconducting transitions. Despite a range of over 4 decades of resistivity at T_c in different compounds, high-T_c cuprates stand out with the most prominent superconducting fluctuations, by a large margin. Within the four listed cuprate families, superconducting fluctuation in $Bi_2Sr_2CaCu_2O_{8+\delta}$ (Bi-2212) is the most prominent [Fig. 1(b)].

Strong superconducting fluctuation has been interpreted as a consequence of quasi-two-dimensionality and correlation-induced low carrier density in the underdoped (UD) to optimally doped (OP) cuprates [17–20]. In these systems, carrier kinetic energy is low due to strong on-site Coulomb repulsion, and an in- or out-of-plane resistive anisotropy as high as $\rho_c/\rho_{ab} \sim 10^5$–$10^6$ has been observed [21,22]. Both aspects jeopardize the mean-field premise of the BCS theory, and provide basis for superconducting fluctuations. In this regime, it is the condensation of Cooper pairs—establishment of phase coherence—that determines T_c. Moreover, the normal state of UD and OP cuprates exhibits pseudogap and strange metal behaviors due to strong electronic correlation. It no longer hosts quasiparticles with well-defined energy-momentum relation stretching the entirety of the Fermi surface, undermining the Cooper instability necessary for BCS pairing [23]. More hole doping is shown to gradually restore quasiparticles to the normal state from the nodal direction toward the antinodal direction [24]. After a critical doping p_c is surpassed, the normal state regains spectral coherence [14], mode-coupling signature becomes rapidly weakened [25], and the superconducting gap-to-T_c ratio starts to evolve toward the weak-coupling d-wave BCS limit [24].

Indeed, transport [26,27], thermodynamic [13], and single-particle probes [14,28–30] all seem to point toward a more three-dimensional, carrier-rich metallic normal state in overdoped cuprates. This leads to a widely held belief that the BCS paradigm has a chance to succeed here. Therefore, it is quite a surprise when recent measurements show that it is also phase coherence that determines T_c in overdoped $(La,Sr)_2CuO_4$ (LSCO) [31–33]. Scanning tunneling spectroscopy (STS) indicates substantial nanoscale electronic inhomogeneity in overdoped Bi-2212, signifying the important role of disorder [34,35]. Photoemission evidence of fluctuating superconductivity has been observed in optimally doped [36] and overdoped cuprates [37], albeit mostly near the more coherent nodal direction. It remains unclear whether such a residual gap above T_c is truly of superconducting origin, or is a vestigial presence of the incoherent pseudogap and/or more exotic gapped states [14,38–41]. The ambiguity on the nature of the antinodal spectral gap above T_c in overdoped cuprates inadvertently created incompatible boundaries trisecting the pseudogap, superconductivity, and normal metal phases [42]. Last but not least, concerted electrical, magnetic, thermodynamic, and single-particle measurements on the same overdoped samples have been lacking, lending much

uncertainty to conclusions pieced together from different cuprate families.

Motivated by these puzzles, we carry out a multitechnique investigation on one cuprate system Bi-2212, aiming to answer the following questions pertinent to overdoped cuprates and beyond.

(1) Is there any residual "pseudogap" that is not of superconducting origin in overdoped cuprates?
(2) How do the transport, thermodynamic, magnetic, and single-particle properties of the normal and superconducting states come together on the same model system Bi-2212?
(3) What may suppress the superfluid density and phase stiffness despite the high carrier density in the overdoped regime?
(4) Will superconducting phase coherence imprint on the single-particle spectral function in this case?

II. MATERIAL SYNTHESIS AND CHARACTERIZATION

Overdoped bilayer cuprate $(Pb,Bi)_2Sr_2CaCu_2O_{8+\delta}$ (Pb: Bi-2212) is chosen for its excellent cleavability and large superconducting energy scale. Pressurized oxygen annealing from 2 to 400 bar is used to reach $66 > T_c > 51$ K, which corresponds to nominal hole doping of $0.22 < p < 0.24$ [43]. Figure 2 shows the magnetic, electrical transport, and thermodynamic signatures of a superconducting transition at $T_c = 66$ K ($p = 0.22$). A sharp superconducting transition defined by the Meissner diamagnetism [Fig. 2(a)] coincides to within 1 K with the zero-resistivity temperature [Fig. 2(b)] and the singularity in both the in-plane lattice expansivity [Fig. 2(c)] and heat capacity [Fig. 2(d)]. A linear background is subtracted from the lattice expansivity and heat capacity data to highlight the transition [44]. Compared to the optimally doped system [22,46], here the out-of-plane and in-plane magnetization anisotropy M_c/M_{ab} is reduced from 1400 to 12, while the corresponding resistivity anisotropy ρ_c/ρ_{ab} is reduced from 10^5 to 600. This suggests a rapid restoration toward three dimensionality with 22% hole doping in both the superconducting and normal states. The thermodynamic singularities are consistent with a sharp second-order superconducting phase transition across T_c. But the extended critical region up to 20 K above T_c signal substantial thermal fluctuations that cannot be rationalized within a simple BCS mean-field picture.

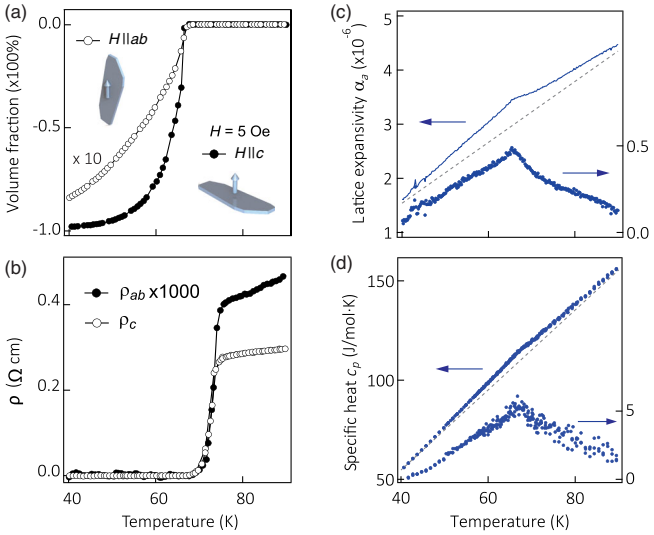

FIG. 2. Bulk magnetic and thermodynamic properties of a heavily overdoped Bi-2212 with $T_c = 66$ K. (a) dc diamagnetic response at 5 Oe, for fields both perpendicular (solid circles) and parallel (open circles) to the CuO_2 plane. (b) In- and out-of-plane resistivity near T_c. (c) In-plane linear lattice expansion coefficient α. (d) Molar specific heat c_p. In both (c) and (d), a linear background (gray dashed line) is removed to highlight the superconducting transition in the bottom curve plotted to the right axes on an enlarged scale.

III. SPECTROSCOPIC RESULTS

To obtain spectroscopic insight, we investigate the same system near the SC gap opening temperature (T_{gap}) and the zero-resistivity temperature (T_c) using high-resolution angle-resolved photoemission spectroscopy (ARPES) and ^{63}Cu nuclear magnetic resonance (NMR) [16]. Systematic high-resolution ARPES measurements in this temperature and doping regime are made possible by the recent advance in localized heating method [14,37], which is instrumental to maintain the surface doping level in such superoxygenated samples (see also Fig. S6 in Supplemental Material for temperature cycles [16]).

First, well-defined single-particle spectral peaks are found over the untruncated normal state Fermi surface well above T_c [Figs. 3(a) and 3(j) herein and Fig. S8 in Supplemental Material [16]], indicating a more metallic normal state compared to OP samples [14]. Experimentally fitted Fermi surface volumes yield an averaged doping of $p = 0.26$ between the bonding and antibonding sheets ($p_{AB} = 0.34$, $p_{BB} = 0.18$), slightly larger than the doping deduced from the empirical parabolic T_c-p relation [40,43,47]. Subsequent discussions will mainly focus on the antibonding band, whose van Hove singularity (VHS) is observed to lie in extreme vicinity of the Fermi level [49,50].

To determine T_{gap}, a high statistics energy-momentum cut along the Brillouin zone (BZ) boundary [red line in Fig. 3(a)] is measured between 10 and 150 K [Figs. 3(b)–3(j)] with an energy resolution of 8 meV. The Fermi function is divided from the spectra to reveal the unoccupied states [for detailed procedures, see Figs. S6 and S7, and for raw energy distribution curves (EDCs), see Fig. S13 [16]]. Enabled by excellent statistics and resolution, both the electron and hole branches of the Bogoliubov quasiparticle dispersions can be traced out around T_c [Fig. 3(k)]. The superconducting gap decreases from 10 K up to 63 K, yet a sizable spectral gap

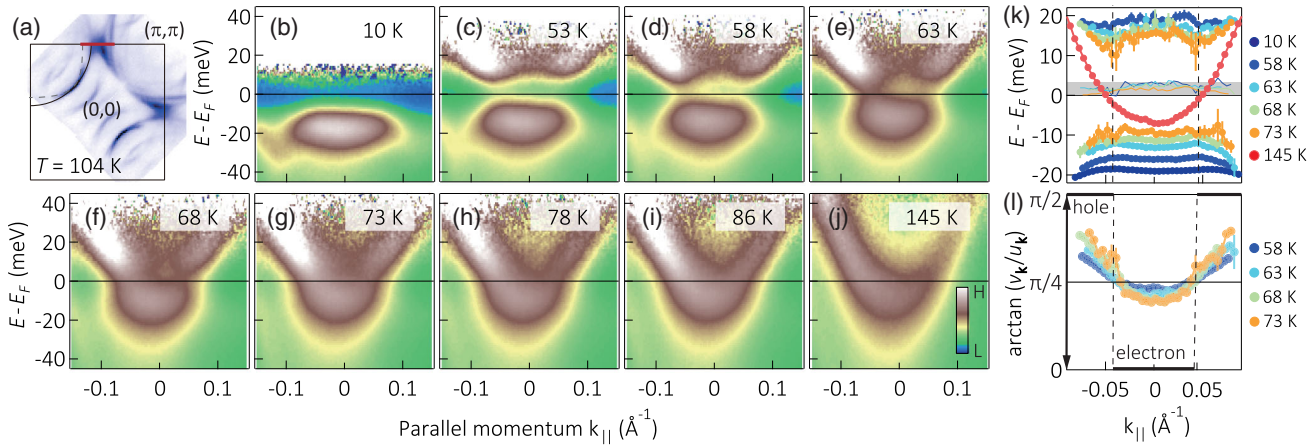

FIG. 3. Temperature-dependent high-resolution antinodal energy-momentum spectra in heavily overdoped Bi-2212 with $T_c = 66$ K. (a) Fermi surface map integrated within 10 meV of the chemical potential of a Pb-free sample in the normal state. Red bar denotes the parallel momentum of the spectra shown in subsequent panels. (b)–(j) Fermi-function-divided antinodal spectra along the BZ boundary in a Pb-doped sample. (k) Fitted energy-momentum dispersions of both the electron and hole Bogoliubov quasiparticles at various temperatures. Red circles indicate the normal state dispersion at 145 K. Thin lines shaded in gray are the averaged energies of the electron and hole Bogoliubov quasiparticle branches. Vertical dashed lines denote the Fermi momenta and gap minima momenta. (l) Calculated particle-hole mixing ratio, expressed in its arc tangent value, from the fitted intensity ratio of the electron and hole Bogoliubov quasiparticle branches near T_c. $\pi/4$ represents equal particle-hole mixture. Black line shows the BCS expectation when $\mathbf{v}_F \cdot \mathbf{k}_F \gg \Delta$.

remains at T_c (cyan markers). In fact, above T_c it continues to close and fill up until it becomes indiscernible around 86 K. During this process, the particle-hole symmetry—evidenced by the dispersion [Fig. 3(k)] and intensity [Fig. 3(l)] of electron and hole branches of the Bogoliubov quasiparticles—remains preserved down to 1.5 meV uncertainty [gray band in Fig. 3(k)], which is quantitatively accountable by the finite resolution effect (Fig. S7 [16]). Such symmetry is also revealed by the alignment between normal state k_F and superconducting gap minima momentum [Fig. 3(k)], and consistently confirmed on the bonding band (Fig. S15 [16]). This particle-hole symmetric normal state gap suggests the presence of Cooper pairing beyond the nodal region [37], and is fundamentally different from the incoherent, particle-hole asymmetric pseudogap in the UD and OP cuprates that competes with superconductivity (Figs. S14 and S15 [16]) [14,51]. A uniformly closing d-wave gap over the entire momentum space upon warming to T_{gap} also disfavors nonzero momentum pairing in this temperature range (Fig. S8 [16]).

To quantify the particle-hole mixing near the antinodal region, Fig. 3(l) shows the Bogoliubov angle [52] $\theta_{\mathbf{k}} = \tan^{-1}|v_{\mathbf{k}}/u_{\mathbf{k}}|$ for temperatures near T_c. Here, $u^2_{\mathbf{k}}(v^2_{\mathbf{k}})$ are the quasiparticle spectral intensities below and above the Fermi energy. Accordingly, $\theta_{\mathbf{k}} = 0$, $\pi/2$ and $\pi/4$ indicate pure electron (particle), pure hole, and equal particle-hole mixture, respectively. For conventional superconductors $\theta_{\mathbf{k}}$ only deviates from 0 or $\pi/2$ in the vicinity of Fermi momenta $\mathbf{k}_F$, since $\Delta/E_F \ll 1$. However, in overdoped Bi-2212 $\theta_{\mathbf{k}}$ is centered around $\pi/4$ for the entire Bogoliubov quasiparticle band around the antinode. We attribute this to the flatness of the normal state antinodal dispersion in comparison to the size of the superconducting gap [53].

We then show that both T_c and T_{gap} can be uniquely determined from the same set of single-particle spectra. The electronic structure undergoes three distinct stages of evolution as a function of temperature. Figures 4(a) and 4(b) track the temperature dependence of the energy distribution curve at the antinodal $\mathbf{k}_F$ and $(\pi, 0)$ on the antibonding band. (1) Cooling toward ~90 K (green lines), the spectral peak gradually sharpens in width and grows in height [for the full temperature range up to 290 K, see Fig. S11(a) [16]]. (2) An energy gap gradually opens below T_{gap}. It starts as the zero-energy spectral intensity saturates, which then further splits into two largely overlapping peaks at T_c (red lines). (3) Further cooling from T_c instigates a rapid sharpening of the Bogoliubov quasiparticle peak, as well as a concomitant rapid depletion of the zero-energy spectral weight until a near-complete energy gap forms. Figures 4(c) and 4(d) quantitatively describe the temperature evolution of the superconducting gap size and spectral peak height (minimally fitted by a Gaussian between −20 and 1 meV) at the antinodal $\mathbf{k}_F$ and $(\pi, 0)$. In particular, taking advantage of the shallow van Hove point, the superconducting gap at $(\pi, 0)$ may be extracted with excellent numerical stability via subtraction of quadrature $\Delta_{\mathbf{k}} = \sqrt{E^2_{\mathbf{k}} - \epsilon^2_{\mathbf{k}}}$ [Fig. 4(c), blue circles; see also Fig. S11 for simulations explaining the difference between results at k_F and $(\pi, 0)$ [16]]. $E_{\mathbf{k}}$ and $\epsilon_{\mathbf{k}}$ are superconducting state and normal state quasiparticle dispersions.

While the momentum resolved single particle spectra most clearly show both T_{gap} and T_c, the onset of

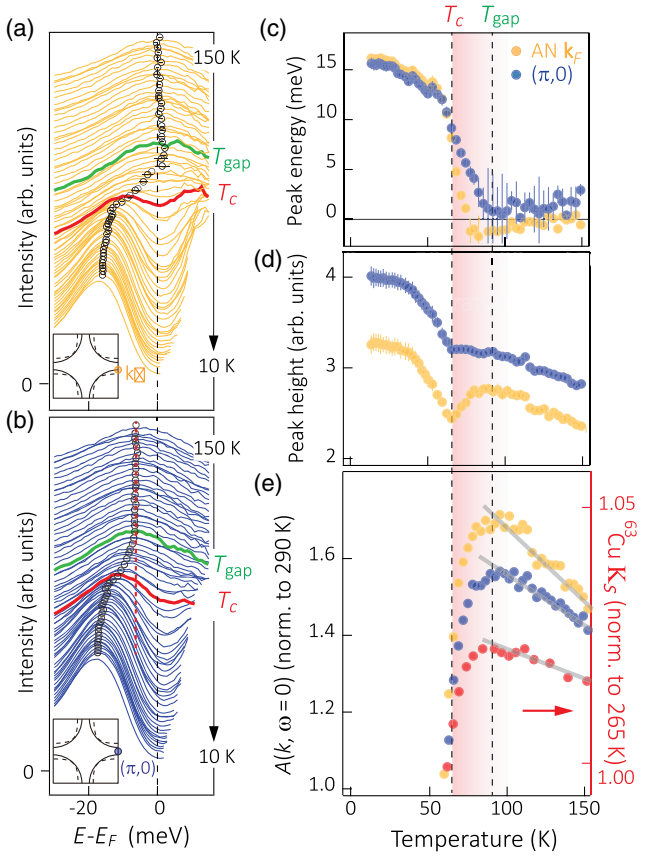

FIG. 4. Temperature dependence of the antinodal EDCs. Fermi-function-divided EDCs at (a) antinodal $\mathbf{k}_F$ and (b) $(\pi, 0)$. Insets depict the two momenta in the Brillouin zone. Spectra are normalized to 1 over [0, 100] meV binding energy. Green and red lines denote $T_{gap} \sim 90$ K and $T_c \sim 66$ K, respectively. Black circles mark the apparent spectral peak position, and the red dashed line marks the ungapped van Hove point position. Temperature-dependent (c) spectral peak binding energy, (d) spectral peak height, and (e) spectral intensity at E_F from the antinodal $\mathbf{k}_F$ (yellow) and $(\pi, 0)$ (blue). Right-hand axis in (e) corresponds to the frequency shift from the ^{63}Cu nuclear spin resonance (red). Gray lines are guides to exemplify normal state spectral weight evolution. Curves in (d) are offset for clarity.

zero-energy spectral weight depletion also signifies T_{gap} [Fig. 4(e)]. This is true both near the antinode shown by the maximum $A(k, \omega = 0)$ in ARPES (blue and yellow circles) and as a momentum average shown by the maximum Knight shift of the ^{63}Cu nuclear magnetic resonance (red circles). The fact that bulk probes, such as NMR, yield results consistent with the surface sensitive ARPES results further supports that the observed fluctuations are a bulk phenomenon [54]. Clearly, there is a mismatch between the bulk gap opening temperature $T_{gap} \sim 87$ K and the bulk superconducting transition temperature $T_c = 66$ K. Intriguingly, replacing T_c with T_{gap} in the superconducting gap-to-T_c ratio $2\Delta(0)/k_B T$, this quantity finally reduces to the weakly coupled d-wave BCS value of ~4.3 [25].

IV. SIGN-PROBLEM-FREE QUANTUM MONTE CARLO SIMULATIONS

So far, upon cooling, our data point to a rather conventional gap opening process intervened by strong phase fluctuations until coherence is achieved. This is consistent with the surprising observation of low zero temperature superfluid density in overdoped LSCO [32]. However, the microscopic mechanism underlying the low superfluid density is unclear. Electronic inhomogeneity and disorder is a natural candidate to disrupt the phase coherence in this regime. But prevalent phase fluctuations in virtually all cuprate families, which have drastically different disorder levels, seem to suggest additional mechanisms [55,56]. Mean-field models of dirty d-wave superconductors account for the reduction of zero temperature superfluid density [57,58]. However, the dirty limit is hard to reach with the extremely short superconducting coherence length [33,45], and the model does not produce notable thermal fluctuations. Here we explore another factor which also contributes to the superfluid density reduction, namely, the flat dispersion near the antinode. To test the viability of this proposal, we study a model system with a similar flat dispersion in the absence of disorder.

It is well known that a flat band comes with a large effective mass, hence low superfluid density or phase stiffness $\sim(n/m^*)$. However, for overdoped cuprates, the band dispersion is only flat near the antinode. This raises the interesting question of what the effect on superfluid density will be if flat band dispersion only exists in part of the Brillouin zone. We address this question with a sign-problem-free quantum Monte Carlo simulation on similar band structure as the overdoped cuprates.

To get rid of the fermion sign problem, and still maintain the strongest pairing interaction at the antinode, we choose a model where the band structure is tuned to mimic that of an overdoped cuprate, while the pairing interaction is mediated by a d-form factor (B_{1g}) Einstein phonon coupled at $\lambda = 0.25$. The reason we choose to simulate the B_{1g}-mediated pairing is threefold. (1) It captures the anisotropic pairing of the cuprates (larger antinodal gap). (2) The resulting pairing problem is computable using sign-problem-free quantum Monte Carlo simulation on a 2D lattice, which is an approximation-free method. (3) Although it does not capture the phase of the gap function, in the absence of disorder, it captures the fact that the SC gap is comparable with antinodal electron band energy, which we believe plays an important role in enhancing the SC fluctuations. We compare the quantum Monte Carlo results for band structures without and with a flat antinodal dispersion. The chosen dispersions [near $(\pi, 0)$] are shown in Figs. 5(a) and 5(b) [experimental band structure is shown in Fig. 5(c)]. In both cases, the system exhibits highly anisotropic s-wave superconducting ground states with the gap maximum at $(\pi, 0)$.

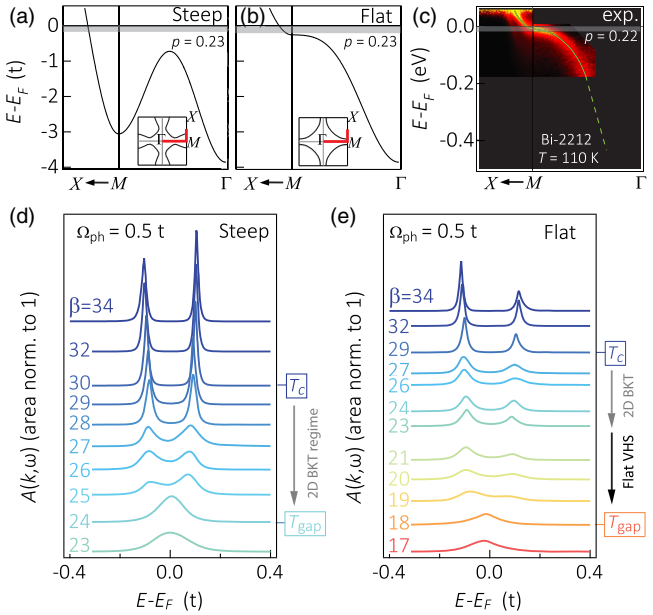

FIG. 5. Band structure contribution to the superconducting fluctuation examined by quantum Monte Carlo simulations. Tight-binding band structures with (a) a steep dispersion and (b) a shallow and flat dispersion near $(\pi, 0)$. The along high symmetry cuts are shown by red lines on their respective Fermi surfaces in the insets. (c) Experimentally measured normal state spectra along the same high symmetry cuts for $p = 0.22$ samples. Gray bars are the superconducting gap sizes. Calculated temperature-dependent single-particle spectra at the antinode for (d) the steep dispersion and (e) the shallow flat dispersion, when anisotropic superconductivity is induced by a B_{1g} phonon. Spectral intensity is normalized so the total area is 1. The curves are offset proportional to temperature $T = 1/\beta$. The electron-phonon coupling strength λ is set to 0.25. $t = 1$ eV is the hopping energy used in the tight-binding model.

Figures 5(d) and 5(e) plot temperature-dependent EDCs near the antinode for band structures shown in Figs. 5(a) and 5(b), respectively [59]. The superconducting gap opening temperature T_{gap}, identified by the closure of the antinodal spectral gap, is 33% higher in the case where the band structure is flat in the antinodal region. This is because the pairing interaction mediated by the B_{1g} phonon can take advantage of the large density of states where flat band exists. On the other hand, the Berezinskii–Kosterlitz–Thouless (BKT) T_c for a band structure with a flat antinodal dispersion is only 3% higher (see Fig. S5 for T_c determination [16]), leaving a much wider temperature window where the gap has opened but phase coherence has yet to be established. Consistent with the enhanced thermal fluctuations above T_c, the zero temperature superfluid density—the quantity central to previous magnetic and optical investigations [32,33]—is 45% lower with the flat dispersion with quantum fluctuations considered [60]. These results suggest that even without disorder, the flat dispersion near the antinode plays an important role in suppressing the superfluid density (or the normal state Drude weight) in clean systems. Additionally, our simulation shows how the superconducting quasiparticle peak only rapidly grows as the global phase coherence is established. While more microscopic theories are clearly needed to understand how global phase coherence can imprint itself on the single-particle spectral properties [61], our work adds insight to a growing number of similar observations in other superconducting systems [62–64].

V. DISCUSSIONS

Real systems always contain disorder, which is also expected to suppress the superfluid density via the breaking of Galilean invariance [65]. In this regard, the flat band dispersion amplifies the effect of disorder via increased scattering between antinodes, which is pair breaking due to the d-wave symmetry [66]. Recent low-temperature STS studies in heavily overdoped $Bi_2Sr_2Ca_2Cu_3O_{10+\delta}$ also indicate the presence of such strong (π, π) scattering [67,68]. Hence the flat dispersion and disorder can have a combined role in driving the superconductor-to-metal transition in the heavily hole-doped cuprates [60]. The answer to which effect is dominant will likely vary between different families of compounds. To verify this proposal further, one may consider direct measurements of phonon or magnetic scattering in the (π, π) channel, or quasiparticle interference via STS, or tuning the van Hove point in different overdoped cuprate compounds.

Our results also emphasize the impact of the low-energy electronic anisotropy on the transport and superconducting properties. While it has become customary to use the Fermi energy E_F as a liaison to describe the carrier density and Drude weight in metallic systems, nonparabolic and anisotropic low-energy electronic structures can cause superconducting fluctuations of dramatically different strengths in systems with identical E_F. As such, plain ratios such as T_c/T_F or Δ/E_F should be used with caution to categorize a material's superconducting properties, especially in the absence of detailed knowledge of its low-energy electronic structures. In heavily hole-doped cuprate superconductors, despite vastly different disorder levels across different families, the ubiquitously shallow van Hove point and its coincidence with the maximum d-wave pairing gap may be one common thread underlying the cuprates' much stronger superconducting fluctuations compared to other bulk superconductors (Fig. 1). Compared to the antibonding band discussed here, the bonding band in Bi-2212 contributes much lower density of states near E_F, which is also much less doping dependent. Therefore, it is considered less central to the fluctuation enhancement scenario.

In summary, we show in this work that despite the much improved three dimensionality and metallicity in a heavily overdoped cuprate, not only is there a persistent spectral gap, but it is also of purely superconducting nature rather than a continuation of the competing pseudogap from the

underdoped cuprates. We find that a shallow, flat van Hove singularity can exacerbate the destruction of phase coherence by itself or together with disorder. We also provide additional experimental and numerical connections between the global phase coherence and the single-particle spectral function. Given the generality of our model, it is plausible that the cooperative effects of flat band and disorder can play a role in the fluctuating phenomena in other systems, such as twisted graphene systems [69] and the nickelates [70,71]. In practice, our results provide not only clear band structure targets to engineer the phase stiffness, but also the basis for T_c enhancement at the interface between superconductors with strong pairing and those with large phase stiffness [72].

ACKNOWLEDGMENTS

The authors wish to thank Steve Kivelson, Edwin Huang, Yao Wang, Junfeng He, Douglas Scalapino, Yoni Schattner, Jiecheng Zhang, Erik Kountz, Rudi Hackl, Peter Hirschfeld, and Jan Zaanen for helpful discussions. The works at Stanford University and Stanford Synchrotron Radiation Lightsource, SLAC National Accelerator Laboratory, are supported by the U.S. Department of Energy, Office of Science, Office of Basic Energy Sciences under Contract No. DE-AC02-76SF00515. Part of this work is performed at the Stanford Nano Shared Facilities (SNSF), supported by the National Science Foundation under Grant No. ECCS-1542152. The works at the University of California, Berkeley and Lawrence Berkeley National Laboratory are supported by U.S. Department of Energy, Office of Science, Office of Basic Energy Sciences, Materials Sciences and Engineering Division under Contract No. DE-AC02-05-CH11231 within the Quantum Materials Program (KC2202). The computational part of this research is supported by the U.S. Department of Energy, Office of Science, Office of Advanced Scientific Computing Research, Scientific Discovery through Advanced Computing (SciDAC) program. T. W. and X.-H. C. acknowledge the support from the National Key R&D Program of the MOST (Grant No. 2017YFA0303001) and the National Natural Science Foundation of China (Grant No. 11888101). D.-H. L. acknowledges support from the Gordon and Betty Moore Foundation's EPiQS initiative Grant No. GBMF4545. Y. H. acknowledges support from the Miller Institute for Basic Research in Science.

[1] J. Bardeen, L. N. Cooper, and J. R. Schrieffer, *Theory of Superconductivity*, Phys. Rev. **108**, 1175 (1957).

[2] V. L. Ginzburg, *Some Remarks on Phase Transitions of the Second Kind and the Microscopic Theory of Ferroelectric Materials*, Fiz. Tverd. Tela (Leningrad) **2**, 2031 (1960) [, Sov. Phys. Solid State **2**, 1824 (1960)].

[3] *Clean* here means the normal state mean free path l_{MFP} is larger than the superconducting coherence length ξ_{BCS}.

[4] C. A. Shiffman, J. F. Cochran, and M. Garber, *The Specific Heat Jump in Superconducting Lead*, J. Phys. Chem. Solids **24**, 1369 (1963).

[5] A. T. Hirshfeld, H. A. Leupold, and H. A. Boorse, *Superconducting and Normal Specific Heats of Niobium*, Phys. Rev. **127**, 1501 (1962).

[6] D. C. Rorer, H. Meyer, and R. C. Richardson, *Specific Heat of Aluminum Near Its Superconductive Transition Point*, Z. Naturforsch. A **18**, 130 (1963), https://zfn.mpdl.mpg.de/data/Reihe_A/18/ZNA-1963-18a-0130.pdf.

[7] B. Sacepe, C. Chapelier, T. I. Baturina, V. M. Vinokur, M. R. Baklanov, and M. Sanquer, *Pseudogap in a Thin Film of a Conventional Superconductor*, Nat. Commun. **1**, 140 (2010).

[8] M. Mondal, A. Kamlapure, M. Chand, G. Saraswat, S. Kumar, J. Jesudasan, L. Benfatto, V. Tripathi, and P. Raychaudhuri, *Phase Fluctuations in a Strongly Disordered s-Wave NbN Superconductor Close to the Metal-Insulator Transition*, Phys. Rev. Lett. **106**, 047001 (2011).

[9] Z. Hao, A. M. Zimmerman, P. Ledwith, E. Khalaf, D. Haie Najafabadi, K. Watanabe, T. Taniguchi, A. Vishwanath, and P. Kim, *Electric Field–Tunable Superconductivity in Alternating-Twist Magic-Angle Trilayer Graphene*, Science **371**, 1133 (2021).

[10] Y. Cao, D. Chowdhury, D. Rodan-Legrain, O. Rubies-Bigorda, K. Watanabe, T. Taniguchi, T. Senthil, and P. Jarillo-Herrero, *Strange Metal in Magic-Angle Graphene with Near Planckian Dissipation*, Phys. Rev. Lett. **124**, 076801 (2020).

[11] B. D. Faeth, S. Yang, J. K. Kawasaki, J. N. Nelson, P. Mishra, L. Chen, D. G. Schlom, and K. M. Shen, *Incoherent Cooper Pairing and Pseudogap Behavior in Single-Layer* $\mathrm{FeSe/SrTiO_3}$, Phys. Rev. X **11**, 021054 (2021).

[12] A. Larkin and A. Varlamov, *Theory of Fluctuations in Superconductors* (Clarendon Press, Oxford, 2005).

[13] J. L. Tallon, J. G. Storey, and J. W. Loram, *Fluctuations and Critical Temperature Reduction in Cuprate Superconductors*, Phys. Rev. B **83**, 092502 (2011).

[14] S.-D. Chen, M. Hashimoto, Y. He, D. Song, K.-J. Xu, J.-F. He, T. P. Devereaux, H. Eisaki, D.-H. Lu, J. Zaanen *et al.*, *Incoherent Strange Metal Sharply Bounded by a Critical Doping in Bi2212*, Science **366**, 1099 (2019).

[15] J. M. Kosterlitz and D. J. Thouless, *Ordering, Metastability and Phase Transitions in Two-Dimensional Systems*, J. Phys. C **6**, 1181 (1973).

[16] See Supplemental Material at http://link.aps.org/supplemental/10.1103/PhysRevX.11.031068 for extended sample characterization, experimental configuration and conditions, numerical simulation details, raw data plot, and the discussion of the procedures for superconducting gap analysis.

[17] J. Corson, R. Mallozzi, J. Orenstein, J. N. Eckstein, and I. Bozovic, *Vanishing of Phase Coherence in Underdoped* $\mathrm{Bi_2Sr_2CaCu_2O_{8+\delta}}$, Nature (London) **398**, 221 (1999).

[18] A. T. Bollinger, G. Dubuis, J. Yoon, D. Pavuna, J. Misewich, and I. Božović, *Superconductor–Insulator Transition in* $\mathrm{La_{2-x}Sr_xCuO_4}$ *at the Pair Quantum Resistance*, Nature (London) **472**, 458 (2011).

[19] Y. J. Uemura, G. M. Luke, B. J. Sternlieb, J. H. Brewer, J. F. Carolan, W. N. Hardy, R. Kadono, J. R. Kempton,

R. F. Kiefl, S. R. Kreitzman *et al.*, *Universal Correlations between T_c and n_s/m^* (Carrier Density over Effective Mass) in High-T_c Cuprate Superconductors*, Phys. Rev. Lett. **62**, 2317 (1989).

[20] V. J. Emery and S. A. Kivelson, *Importance of Phase Fluctuations in Superconductors with Small Superfluid Density*, Nature (London) **374**, 434 (1995).

[21] S. Ono and Y. Ando, *Evolution of the Resistivity Anisotropy in $Bi_2Sr_{2-x}La_xCuO_{6+\delta}$ Single Crystals for a Wide Range of Hole Doping*, Phys. Rev. B **67**, 104512 (2003).

[22] X. H. Chen, M. Yu, K. Q. Ruan, S. Y. Li, Z. Gui, G. C. Zhang, and L. Z. Cao, *Anisotropic Resistivities of Single-Crystal $Bi_2Sr_2CaCu_2O_{8+\delta}$ with Different Oxygen Content*, Phys. Rev. B **58**, 14219 (1998).

[23] T. A. Maier, P. Staar, V. Mishra, U. Chatterjee, J. C. Campuzano, and D. J. Scalapino, *Pairing in a Dry Fermi Sea*, Nat. Commun. **7**, 11875 (2016).

[24] J. A. Sobota, Y. He, and Z.-X. Shen, *Electronic Structure of Quantum Materials Studied by Angle-Resolved Photoemission Spectroscopy*, Rev. Mod. Phys. **93**, 025006 (2021).

[25] Y. He, M. Hashimoto, D. Song, S.-D. Chen, J. He, I. M. Vishik, B. Moritz, D.-H. Lee, N. Nagaosa, J. Zaanen *et al.*, *Rapid Change of Superconductivity and Electron-Phonon Coupling through Critical Doping in Bi-2212*, Science **362**, 62 (2018).

[26] Y. Ando, S. Komiya, K. Segawa, S. Ono, and Y. Kurita, *Electronic Phase Diagram of High-T_c Cuprate Superconductors from a Mapping of the In-Plane Resistivity Curvature*, Phys. Rev. Lett. **93**, 267001 (2004).

[27] C. Proust, E. Boaknin, R. W. Hill, L. Taillefer, and A. P. Mackenzie, *Heat Transport in a Strongly Overdoped Cuprate: Fermi Liquid and a Pure d-Wave BCS Superconductor*, Phys. Rev. Lett. **89**, 147003 (2002).

[28] Z. M. Yusof, B. O. Wells, T. Valla, A. V. Fedorov, P. D. Johnson, Q. Li, C. Kendziora, S. Jian, and D. G. Hinks, *Quasiparticle Liquid in the Highly Overdoped $Bi_2Sr_2CaCu_2O_{8+\delta}$*, Phys. Rev. Lett. **88**, 167006 (2002).

[29] Y.-D. Chuang, A. D. Gromko, A. V. Fedorov, Y. Aiura, K. Oka, Y. Ando, M. Lindroos, R. S. Markiewicz, A. Bansil, and D. S. Dessau, *Bilayer Splitting and Coherence Effects in Optimal and Underdoped $Bi_2Sr_2CaCu_2O_{8+\delta}$*, Phys. Rev. B **69**, 094515 (2004).

[30] K. Fujita, C. K. Kim, I. Lee, J. Lee, M. H. Hamidian, I. A. Firmo, S. Mukhopadhyay, H. Eisaki, S. Uchida, M. J. Lawler *et al.*, *Simultaneous Transitions in Cuprate Momentum-Space Topology and Electronic Symmetry Breaking*, Science **344**, 612 (2014).

[31] P. M. C. Rourke, I. Mouzopoulou, X. Xu, C. Panagopoulos, Y. Wang, B. Vignolle, C. Proust, E. V. Kurganova, U. Zeitler, Y. Tanabe *et al.*, *Phase-Fluctuating Superconductivity in Overdoped $La_{2-x}Sr_xCuO_4$*, Nat. Phys. **7**, 455 (2011).

[32] I. Božović, X. He, J. Wu, and A. T. Bollinger, *Dependence of the Critical Temperature in Overdoped Copper Oxides on Superfluid Density*, Nature (London) **536**, 309 (2016).

[33] F. Mahmood, X. He, I. Božović, and N. P. Armitage, *Locating the Missing Superconducting Electrons in the Overdoped Cuprates $La_{2-x}Sr_xCuO_4$*, Phys. Rev. Lett. **122**, 027003 (2019).

[34] K. K. Gomes, A. N. Pasupathy, A. Pushp, S. Ono, Y. Ando, and A. Yazdani, *Visualizing Pair Formation on the Atomic Scale in the High-T_c Superconductor $Bi_2Sr_2CaCu_2O_{8+\delta}$*, Nature (London) **447**, 569 (2007).

[35] C. V. Parker, A. Pushp, A. N. Pasupathy, K. K. Gomes, J. Wen, Z. Xu, S. Ono, G. Gu, and A. Yazdani, *Nanoscale Proximity Effect in the High-Temperature Superconductor $Bi_2Sr_2CaCu_2O_{8+\delta}$ Using a Scanning Tunneling Microscope*, Phys. Rev. Lett. **104**, 117001 (2010).

[36] T. Kondo, Y. Hamaya, A. D. Palczewski, T. Takeuchi, J. S. Wen, Z. J. Xu, G. Gu, J. Schmalian, and A. Kaminski, *Disentangling Cooper-Pair Formation above the Transition Temperature from the Pseudogap State in the Cuprates*, Nat. Phys. **7**, 21 (2011).

[37] T. Kondo, W. Malaeb, Y. Ishida, T. Sasagawa, H. Sakamoto, T. Takeuchi, T. Tohyama, and S. Shin, *Point Nodes Persisting Far Beyond T_c in Bi2212*, Nat. Commun. **6**, 7699 (2015).

[38] I. M. Vishik, M. Hashimoto, R.-H. He, W.-S. Lee, F. Schmitt, D. Lu, R. G. Moore, C. Zhang, W. Meevasana, T. Sasagawa *et al.*, *Phase Competition in Trisected Superconducting Dome*, Proc. Natl. Acad. Sci. U.S.A. **109**, 18332 (2012).

[39] M. Hashimoto, E. A. Nowadnick, R.-H. He, I. M. Vishik, B. Moritz, Y. He, K. Tanaka, R. G. Moore, D. Lu, Y. Yoshida *et al.*, *Direct Spectroscopic Evidence for Phase Competition between the Pseudogap and Superconductivity in $Bi_2Sr_2CaCu_2O_{8+\delta}$*, Nat. Mater. **14**, 37 (2015).

[40] I. K. Drozdov, I. Pletikosić, C.-K. Kim, K. Fujita, G. D. Gu, J. C. S. Davis, P. D. Johnson, I. Božović, and T. Valla, *Phase Diagram of $Bi_2Sr_2CaCu_2O_{8+\delta}$ Revisited*, Nat. Commun. **9**, 5210 (2018).

[41] Z. Dai, T. Senthil, and P. A. Lee, *Modeling the Pseudogap Metallic State in Cuprates: Quantum Disordered Pair Density Wave*, Phys. Rev. B **101**, 064502 (2020).

[42] A. A. Kordyuk, *Pseudogap from ARPES Experiment: Three Gaps in Cuprates and Topological Superconductivity*, Low Temp. Phys. **41**, 319 (2015).

[43] M. R. Presland, J. L. Tallon, R. G. Buckley, R. S. Liu, and N. E. Flower, *General Trends in Oxygen Stoichiometry Effects on T_c in Bi and Tl Superconductors*, Physica (Amsterdam) **176C**, 95 (1991).

[44] A more involved background subtraction method was carried out in Refs. [13,45], where a nonlinear phonon background from a Zn-doped nonsuperconducting sample was used. Despite the different background subtraction schemes, the extracted mean-field pairing temperature T_{MF} is consistently 30%–40% higher than the resistive transition T_c.

[45] J. W. Loram, J. L. Tallon, and W. Y. Liang, *Absence of Gross Static Inhomogeneity in Cuprate Superconductors*, Phys. Rev. B **69**, 060502 (2004).

[46] G. D. Gu, R. Puzniak, K. Nakao, G. J. Russell, and N. Koshizuka, *Anisotropy of Bi-2212 Superconducting Crystals*, Supercond. Sci. Technol. **11**, 1115 (1998).

[47] It should be noted that the Luttinger volume determined this way may also deviate from the actual filling in the presence of lingering correlation effects [48].

[48] C. Gros, B. Edegger, V. N. Muthukumar, and P. W. Anderson, *Determining the Underlying Fermi Surface of*

Strongly Correlated Superconductors, Proc. Natl. Acad. Sci. U.S.A. **103**, 14298 (2006).

[49] D. S. Dessau, Z.-X. Shen, D. M. King, D. S. Marshall, L. W. Lombardo, P. H. Dickinson, A. G. Loeser, J. DiCarlo, C.-H. Park, A. Kapitulnik, and W. E. Spicer, *Key Features in the Measured Band Structure of* $Bi_2Sr_2CaCu_2O_{8+\delta}$*: Flat Bands at* E_f *and Fermi Surface Nesting*, Phys. Rev. Lett. **71**, 2781 (1993).

[50] A. Kaminski, S. Rosenkranz, H. M. Fretwell, M. R. Norman, M. Randeria, J. C. Campuzano, J. M. Park, Z. Z. Li, and H. Raffy, *Change of Fermi-Surface Topology in* $Bi_2Sr_2CaCu_2O_{8+\delta}$ *with Doping*, Phys. Rev. B **73**, 174511 (2006).

[51] M. Hashimoto, R.-H. He, K. Tanaka, J.-P. Testaud, W. Meevasana, R. G. Moore, D. Lu, H. Yao, Y. Yoshida, H. Eisaki *et al.*, *Particle–Hole Symmetry Breaking in the Pseudogap State of Bi2201*, Nat. Phys. **6**, 414 (2010).

[52] K. Fujita, I. Grigorenko, J. Lee, W. Wang, J. X. Zhu, J. C. Davis, H. Eisaki, S.-I. Uchida, and A. V. Balatsky, *Bogoliubov Angle and Visualization of Particle-Hole Mixture in Superconductors*, Phys. Rev. B **78**, 054510 (2008).

[53] Without a superconducting gap, the van Hove point at $(\pi, 0)$ is only 7 meV below the Fermi energy. All of the electronic states here will be absorbed into the 16 meV superconducting gap well below T_c.

[54] Consistent ARPES and NMR signatures are also observed in even heavier overdoped Bi-2212 (Figs. S3, S4, and S10 of Supplemental Material [16]).

[55] Y. Wang, J. Yan, L. Shan, H.-H. Wen, Y. Tanabe, T. Adachi, and Y. Koike, *Weak-Coupling d-Wave BCS Superconductivity and Unpaired Electrons in Overdoped* $La_{2-x}Sr_xCuO_4$ *Single Crystals*, Phys. Rev. B **76**, 064512 (2007).

[56] I. Božović, J. Wu, X. He, and A. T. Bollinger, *What Is Really Extraordinary in Cuprate Superconductors?*, Physica (Amsterdam) **558C**, 30 (2019).

[57] N. R. Lee-Hone, V. Mishra, D. M. Broun, and P. J. Hirschfeld, *Optical Conductivity of Overdoped Cuprate Superconductors: Application to* $La_{2-x}Sr_xCuO_4$, Phys. Rev. B **98**, 054506 (2018).

[58] N. R. Lee-Hone, H. U. Özdemir, V. Mishra, D. M. Broun, and P. J. Hirschfeld, *Low Energy Phenomenology of the Overdoped Cuprates: Viability of the Landau-BCS Paradigm*, Phys. Rev. Research **2**, 013228 (2020).

[59] The particle-hole asymmetry is due to the small momentum deviation from the exact $\mathbf{k}_F$ in the finite lattice used for the simulation.

[60] Z.-X. Li, S. A. Kivelson, and D.-H. Lee, *Superconductor-to-Metal Transition in Overdoped Cuprates*, npj Quantum Mater. **6**, 1 (2021).

[61] E. W. Carlson, D. Orgad, S. A. Kivelson, and V. J. Emery, *Dimensional Crossover in Quasi-One-Dimensional and High-*T_c *Superconductors*, Phys. Rev. B **62**, 3422 (2000).

[62] D. L. Feng, D. H. Lu, K. M. Shen, C. Kim, H. Eisaki, A. Damascelli, R. Yoshizaki, J.-I. Shimoyama, K. Kishio, G. D. Gu *et al.*, *Signature of Superfluid Density in the Single-Particle Excitation Spectrum of* $Bi_2Sr_2CaCu_2O_{8+\delta}$, Science **289**, 277 (2000).

[63] B. Sacépé, T. Dubouchet, C. Chapelier, M. Sanquer, M. Ovadia, D. Shahar, M. FeigelMan, and L. Ioffe, *Localization of Preformed Cooper Pairs in Disordered Superconductors*, Nat. Phys. **7**, 239 (2011).

[64] D. Cho, K. M. Bastiaans, D. Chatzopoulos, G. D. Gu, and M. P. Allan, *A Strongly Inhomogeneous Superfluid in an Iron-Based Superconductor*, Nature (London) **571**, 541 (2019).

[65] A. J. Leggett *et al.*, *Quantum Liquids: Bose Condensation and Cooper Pairing in Condensed-Matter Systems* (Oxford University Press, New York, 2006).

[66] Y. He, Y. Yin, M. Zech, A. Soumyanarayanan, M. M. Yee, T. Williams, M. C. Boyer, K. Chatterjee, W. D. Wise, I. Zeljkovic *et al.*, *Fermi Surface and Pseudogap Evolution in a Cuprate Superconductor*, Science **344**, 608 (2014).

[67] C. Zou, Z. Hao, X. Luo, S. Ye, Q. Gao, X. Li, M. Xu, P. Cai, C. Lin, X. Zhou *et al.*, *Particle-Hole Asymmetric Superconducting Coherence Peaks in Overdoped Cuprates*, arXiv:2103.06094.

[68] In this case, particle-hole symmetry of the superconducting quasiparticles is locally broken due to (π, π)-scattering induced level splitting on the order of 2–3 meV, which will spatially average to particle-hole symmetric quasiparticle peaks on length scales longer than a few in-plane lattice constants.

[69] X. Liu, Z. Hao, E. Khalaf, J. Y. Lee, Y. Ronen, H. Yoo, D. H. Najafabadi, K. Watanabe, T. Taniguchi, A. Vishwanath *et al.*, *Tunable Spin-Polarized Correlated States in Twisted Double Bilayer Graphene*, Nature (London) **583**, 221 (2020).

[70] D. Li, K. Lee, B. Y. Wang, M. Osada, S. Crossley, H. R. Lee, Y. Cui, Y. Hikita, and H. Y. Hwang, *Superconductivity in an Infinite-Layer Nickelate*, Nature (London) **572**, 624 (2019).

[71] M.-Y. Choi, W. E. Pickett, and K.-W. Lee, *Fluctuation-Frustrated Flat Band Instabilities in* $NdNiO_2$, Phys. Rev. Research **2**, 033445 (2020).

[72] S. A. Kivelson, *Making High* T_c *Higher: A Theoretical Proposal*, Physica (Amsterdam) **318B**, 61 (2002).